

## Chapter 3

# Examples of Chaotic Behaviors

Classical models tell us more than we at first can know.

*Karl Popper (1902–1994)*

In this Chapter, we consider three systems which played a crucial role in the development of dynamical systems theory: the logistic map introduced in the context of mathematical ecology; the model derived by Lorenz (1963) as a simplification of thermal convection; the Hénon and Heiles (1964) Hamiltonian system introduced to model the motion of a star in a galaxy.

### 3.1 The logistic map

Dynamical systems constitute a mathematical framework common to many disciplines, among which ecology and population dynamics. As early as 1798, the Reverend Malthus wrote *An Essay on the Principle of Population* which was a very influential book for later development of population dynamics, economics and evolution theory.<sup>1</sup> In this book, it was introduced a growth model which, in modern mathematical language, amounts to assume that the differential equation  $dx/dt = rx$  describes the evolution of the number of individuals  $x$  of a population in the course of time,  $r$  being the reproductive power of individuals. The Malthusian growth model, however, is far too simplistic as it predicts, for  $r > 0$ , an unbounded exponential growth  $x(t) = x(0) \exp(rt)$ , which is unrealistic for finite-resources environments. In 1838 the mathematician Verhulst, inspired by Malthus' essay, proposed to use the *Logistic equation* to model the self-limiting growth of a biological population:  $dx/dt = rx(1 - x/K)$  where  $K$  is the carrying capacity — the maximum number of individuals that the environment can support. With  $x/K \rightarrow x$ , the above equation can be rewritten as

$$\frac{dx}{dt} = f_r(x) = rx(1 - x), \quad (3.1)$$

---

<sup>1</sup>It is cited as a source of inspiration by Darwin himself.

where  $r(1-x)$  is the normalized reproductive power, accounting for the decrease of reproduction when too many individuals are present in the same limited environment. The logistic equation thus represents a more realistic model. By employing the tools of linear analysis described in Sec. 2.4, one can readily verify that Eq. (3.1) possesses two fixed points:  $x^* = 0$  unstable as  $r > 0$  and  $x^* = 1$  which is stable. Therefore, asymptotically the population stabilizes to a number of individuals equal to the carrying capacity.

The reader may now wonder: Where is chaos? As seen in Sec. 2.3, a one-dimensional ordinary differential equation, although nonlinear, cannot sustain chaos. However, a differential equation to describe population dynamics is not the best model as populations grow or decrease from one generation to the next one. In other terms, a discrete time model, connecting the  $n$ -th generation to the next  $n+1$ -th, would be more appropriate than a continuous time one. This does not make a big difference in the Malthusian model as  $x(n+1) = rx(n)$  still gives rise to an exponential growth ( $r > 1$ ) or extinction ( $0 < r < 1$ ) because  $x(n) = r^n x(0) = \exp(n \ln r)x(0)$ . However, the situation changes for the discretized logistic equation or logistic map:

$$x(n+1) = f_r(x(n)) = rx(n)(1-x(n)), \quad (3.2)$$

which, as seen in Sec. 2.3, being a one-dimensional but non-invertible map may generate chaotic orbits. Unlike its continuous version, the logistic map is well defined only for  $x \in [0:1]$ , limiting the allowed values of  $r$  to the range  $[0:4]$ .

The logistic map is able to produce erratic behaviors resembling random noise for some values of  $r$ . For example, already in 1947 Ulam and von Neumann proposed its use as a random number generator with  $r = 4$ , even though a mathematical understanding of its behavior came later with the works of Ricker (1954) and Stein and Ulam (1964). These works together with other results are reviewed in a seminal paper by May (1976).

Let's start the analysis of the logistic map (3.2) in the linear stability analysis framework. Before that, it is convenient to introduce a graphical method allowing us to easily understand the behavior of trajectories generated by any one-dimensional map. Figure 3.1 illustrates the iteration of the logistic map for  $r = 0.9$  via the following graphical method

- (1) draw the function  $f_r(x)$  and the line bisecting the square  $[0:1] \times [0:1]$ ;
- (2) draw a vertical line from  $(x(0), 0)$  up to intercepting the graph of  $f_r(x)$  in  $(x(0), f_r(x(0)) = x(1))$ ;
- (3) from this point draw a horizontal line up to intercepting the bisecting line;
- (4) repeat the procedure from (2) with the new point.

The graphical method (1)–(4) enables to easily understand the qualitative features of the evolution  $x(0), \dots, x(n), \dots$ . For instance, for  $r = 0.9$ , the bisecting line intersects the graph of  $f_r(x)$  only in  $x^* = 0$ , which is the stable fixed point as  $\lambda(0) = |df_r/dx|_0 < 1$ , which is the slope of the tangent to the curve in 0 (Fig. 3.1).

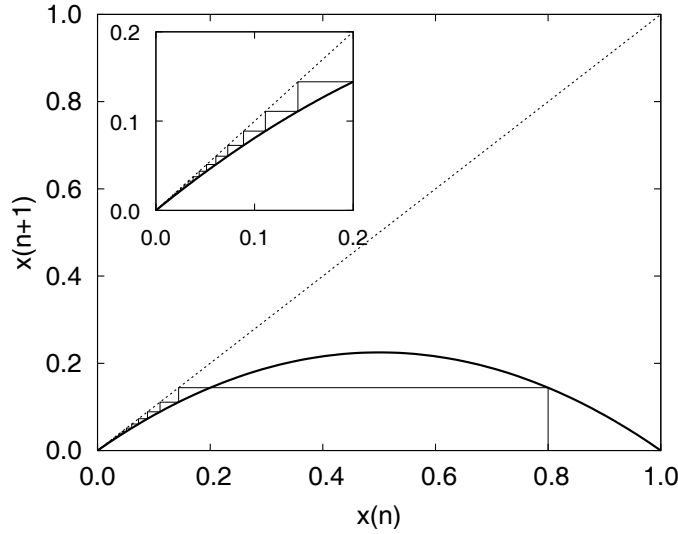


Fig. 3.1 Graphical solution of the logistic map (3.2) for  $r = 0.9$ , for a description of the method see text. The inset shows a magnification of the iteration close to the fixed point  $x^* = 0$ .

Starting from, e.g.,  $x(0) = 0.8$  one can see that few iterations of the map lead the trajectory  $x(n)$  to converge to  $x^* = 0$ , corresponding to population extinction. For  $r > 1$ , the bisecting line intercepts the graph of  $f_r(x)$  in two (fixed) points (Fig. 3.2)

$$x^* = f_r(x^*) \implies x_1^* = 0, x_2^* = 1 - \frac{1}{r}.$$

We can study their stability either graphically or evaluating the map derivative

$$\lambda(x^*) = |f_r'(x^*)| = |r(1 - 2x^*)|, \quad (3.3)$$

where, to ease the notation, we defined  $f_r'(x^*) = df_r(x)/dx|_{x^*}$ . For  $1 < r < 3$ , the fixed point  $x_1^* = 0$  is unstable while  $x_2^* = 1 - 1/r$  is (asymptotically) stable. This means that all orbits, whatever the initial value  $x(0) \in ]0 : 1[$ , will end at  $x_2^*$ , i.e. population dynamics is attracted to a stable and finite number of individuals. This is shown in Fig. 3.2a, where we plot two trajectories  $x(t)$  starting from different initial values. What does happen to the population for  $r > r_1 = 3$ ? For such values of  $r$ , the fixed point becomes unstable,  $\lambda(x_2^*) > 1$ . In Fig. 3.2b, we show the iterations of the logistic map for  $r = 3.2$ . As one can see, all trajectories end in a period-2 orbit, which is the discrete time version of a limit cycle (Sec. 2.4.2). Thanks to the simplicity of the logistic map, we can easily extend linear stability analysis to periodic orbits. It is enough to consider the second iterate of the map

$$f_r^{(2)}(x) = f_r(f_r(x)) = r^2 x(1-x)(1-rx+rx^2), \quad (3.4)$$

which connects the population of the grandmothers with that of the granddaughters, i.e.  $x(n+2) = f_r^{(2)}(x(n))$ . Clearly, a period-2 orbit corresponds to a fixed point of such a map. The quartic polynomial (3.4) possesses four roots

$$x^* = f_r^{(2)}(x^*) \implies \begin{cases} x_1^* = 0, & x_2^* = 1 - \frac{1}{r} \\ x_{3,4}^* = \frac{(r+1) \pm \sqrt{(r+1)(r-3)}}{2r} : \end{cases} \quad (3.5)$$

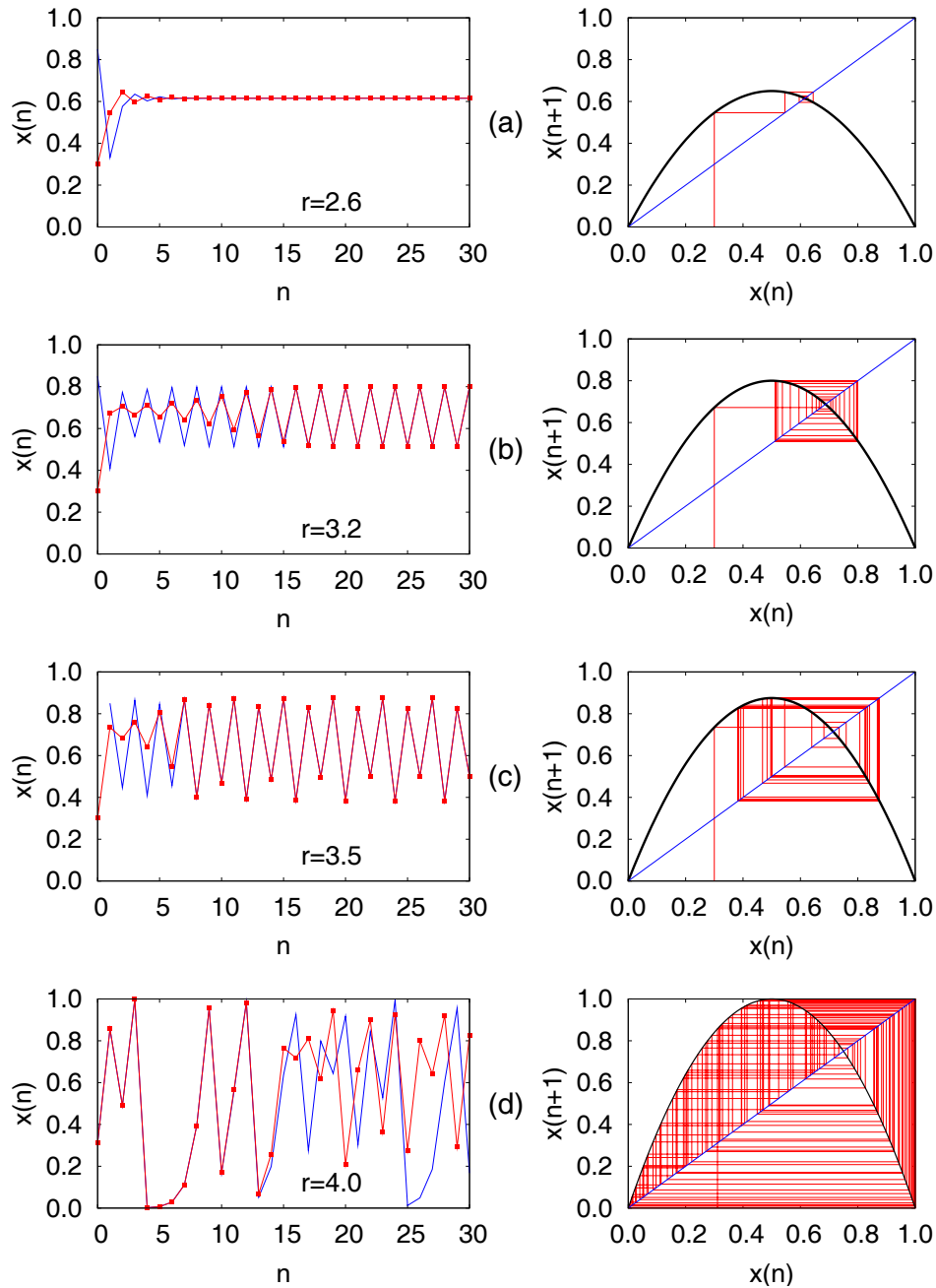


Fig. 3.2 Left: (a) evolution of two trajectories (red and blue) initially at distance  $|x'(0) - x(0)| \approx 0.5$  which converge to the fixed point for  $r = 2.6$ ; (b) same of (a) but for an attracting period-2 orbit at  $r = 3.2$ ; (c) same of (a) but for an attracting period-4 orbit at  $r = 3.5$ ; (d) evolution of two trajectories (red and blue), initially very close  $|x'(0) - x(0)| = 4 \times 10^{-6}$ , in the chaotic regime for  $r = 4$ . Right: graphical solution of the logistic map as explained in the text.

two coincide with the original ones ( $x_{1,2}^*$ ), as an obvious consequence of the fact that  $f_r(x_{1,2}^*) = x_{1,2}^*$ , and two ( $x_{3,4}^*$ ) are new. The change of stability of the fixed points

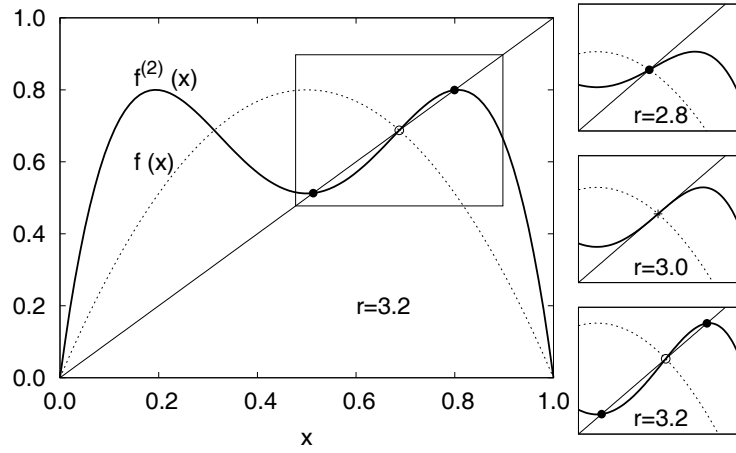


Fig. 3.3 Second iterate  $f_r^{(2)}(x)$  (solid curve) of the Logistic map (dotted curve). Note the three intercepts with the bisecting line, i.e. the three fixed points  $x_2^*$  (unstable open circle) and  $x_{3,4}^*$  (stable in filled circles). The three panels on the right depict the evolution the intercepts from  $r < r_1 = 3$  to  $r > r_1$  as in label.

is shown on the right of Fig. 3.3. For  $r < 3$ , the stable fixed point is  $x_2^* = 1 - 1/r$ . At  $r = 3$ , as clear from Eq. (3.5),  $x_3^*$  and  $x_4^*$  start to be real and, in particular,  $x_3^* = x_4^* = x_2^*$ . We can now compute the stability eigenvalues through the formula

$$\lambda^{(2)}(x^*) = \left| \frac{df_r^{(2)}}{dx} \right|_{x^*} = |f_r'(f_r(x^*)) \cdot f_r'(x^*)| = \lambda(f_r(x^*))\lambda(x^*), \quad (3.6)$$

where the last two equalities stem from the chain rule<sup>2</sup> of differentiation. One thus finds that: for  $r = 3$ ,  $\lambda^{(2)}(x_2^*) = (\lambda(x_2^*))^2 = 1$  i.e. the point is marginal, the slope of the graph of  $f_r^{(2)}$  is 1; for  $r > 3$ , it is unstable (the slope exceeds 1) so that  $x_3^*$  and  $x_4^*$  become the new stable fixed points.

For  $r_1 < r < r_2 = 3.448\dots$ , the period-2 orbit is stable as  $\lambda^{(2)}(x_3^*) = \lambda^{(2)}(x_4^*) < 1$ . From Fig. 3.2c we understand that, for  $r > r_2$ , period-4 orbits become the stable and attracting solutions. By repeating the above procedure to the 4<sup>th</sup>-iterate  $f^{(4)}(x)$ , it is possible to see that the mechanism for the appearance of period-4 orbits from period-2 ones is the same as the one illustrated in Fig. 3.3. Step by step several critical values  $r_k$  with  $r_k < r_{k+1}$  can be found: if  $r_k < r < r_{k+1}$ , after an initial transient,  $x(n)$  evolves on a period- $2^k$  orbit [May (1976)].

The change of stability, at varying a parameter, of a dynamical system is a phenomenon known as *bifurcation*. There are several types of bifurcations which

<sup>2</sup>Formula (3.6) can be straightforwardly generalized for computing the stability of a generic period- $T$  orbit  $x^*(1), x^*(2), \dots, x^*(T)$ , with  $f^{(T)}(x^*(i)) = x^*(i)$  for any  $i = 1, \dots, T$ . Through the chain rule of differentiation the derivative of the map  $f^{(T)}(x)$  at any of the points of the orbit is given by

$$\frac{df^{(T)}}{dx} \Big|_{x^*(1)} = f'(x^*(1)) f'(x^*(2)) \cdots f'(x^*(T)).$$

constitute the basic mechanisms through which more and more complex solutions and finally chaos appear in dissipative dynamical systems (see Chapter 6). The specific mechanism for the appearance of the period- $2^k$  orbits is called *period doubling* bifurcation. Remarkably, as we will see in Sec. 6.2, the sequence  $r_k$  has a limit:  $\lim_{k \rightarrow \infty} r_k = 3.569945 \dots = r_\infty < 4$ .

For  $r > r_\infty$ , the trajectories display a qualitative change of behavior as exemplified in Fig. 3.2d for  $r = 4$ , which is called the Ulam point. The graphical method applied to the case  $r = 4$  suggests that, unlike the previous cases, no stable periodic orbits exist,<sup>3</sup> and the trajectory looks random, giving support to the proposal of Ulam and von Neumann (1947) to use the logistic map to generate random sequences of numbers on a computer. Even more interesting is to consider two initially close trajectories and compare their evolution with that of trajectories at  $r < r_\infty$ . On the one hand, for  $r < r_\infty$  (see the left panel of Fig. 3.2a–c) two trajectories  $x(n)$  and  $x'(n)$  starting from distant values (e.g.  $\delta x(0) = |x(0) - x'(0)| \approx 0.5$ , any value would produce the same effect) quickly converge toward the same period- $2^k$  orbit.<sup>4</sup> On the other hand, for  $r = 4$  (left panel of Fig. 3.2d), even if  $\delta x(0)$  is infinitesimally small, the two trajectories quickly become “macroscopically” distinguishable, resembling what we observed for the driven-damped pendulum (Fig. 1.4). This is again chaos at work: emergence of very irregular, seemingly random trajectories with sensitive dependence on the initial conditions.<sup>5</sup>

Fortunately, in the specific case of the logistic map at the Ulam point  $r = 4$ , we can easily understand the origin of the sensitive dependence on initial conditions. The idea is to establish a change of variable transforming the logistic in a simpler map, as follows. Define  $x = \sin^2(\pi\theta/2) = [1 - \cos(\pi\theta)]/2$  and substitute it in Eq. (3.2) with  $r = 4$ , so to obtain  $\sin^2(\pi\theta(n+1)/2) = \sin^2(\pi\theta(n))$  yielding to

$$\pi\theta(n+1)/2 = \pm\pi\theta(n) + k\pi, \quad (3.7)$$

where  $k$  is any integer. Taking  $\theta \in [0 : 1]$ , it is straightforward to recognize that Eq. (3.7) defines the map

$$\theta(n+1) = \begin{cases} 2\theta(n) & 0 \leq \theta < \frac{1}{2} \\ 2 - 2\theta(n) & \frac{1}{2} \leq \theta \leq 1 \end{cases} \quad (3.8)$$

or, equivalently,  $\theta(n+1) = g(\theta(n)) = 1 - 2|\theta(n) - 1/2|$  which is the so-called *tent map* (Fig. 3.4a).

Intuition suggests that the properties of the logistic map with  $r = 4$  should be the same as those of the tent map (3.8), this can be made more precise introducing the concept of *Topological Conjugacy* (see Box B.3). Therefore, we now focus on the behavior of a generic trajectory under the action of the tent map (3.8), for which

<sup>3</sup>There is however an infinite number of unstable periodic orbits, as one can easily understand plotting the  $n$ -iterates of the map and look for the intercepts with the bisectrix.

<sup>4</sup>Note that the periodic orbit may be shifted of some iterations.

<sup>5</sup>One can check that making  $\delta x(0)$  as small as desired simply shifts the iteration at which the two orbits become macroscopically distinguishable.

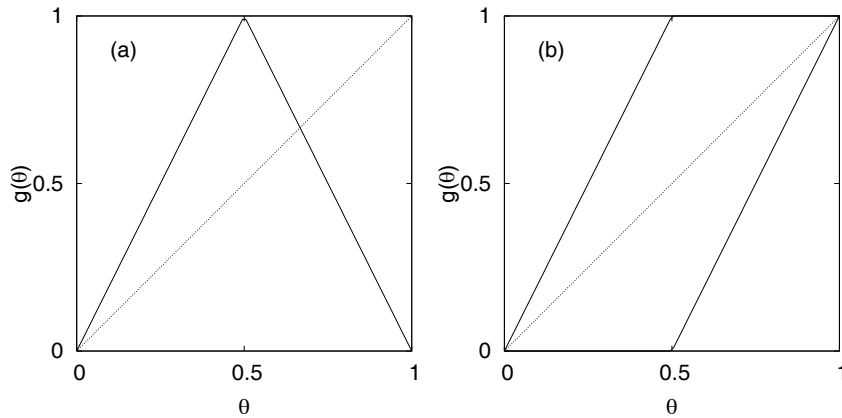


Fig. 3.4 (a) Tent map (3.8). (b) Bernoulli shift map (3.9).

chaos appears in a rather transparent way, so to infer the properties of the logistic map for  $r = 4$ .

To understand why chaos, meant as sensitive dependence on initial conditions, characterizes the tent map, it is useful to warm up with an even simpler instance, that is the *Bernoulli Shift map*<sup>6</sup> (Fig. 3.4b)

$$\theta(n+1) = 2\theta(n) \pmod{1}, \text{ i.e. } \theta(n+1) = \begin{cases} 2\theta(n) & 0 \leq \theta(n) < \frac{1}{2} \\ 2\theta(n) - 1 & \frac{1}{2} \leq \theta(n) < 1, \end{cases} \quad (3.9)$$

which is composed by a branch of the tent map, for  $\theta < 1/2$ , and by its reflection with respect to the line  $g(\theta) = 1/2$ , for  $1/2 < \theta < 1$ . The effect of the iteration of the Bernoulli map is trivially understood by expressing a generic initial condition in binary representation

$$\theta(0) = \sum_{i=1}^{\infty} \frac{a_i}{2^i} \equiv [a_1, a_2, \dots]$$

where  $a_i = 0, 1$ . The action of map (3.9) is simply to remove the most significant digit, i.e. the binary shift operation

$$\theta(0) = [a_1, a_2, a_3, \dots] \rightarrow \theta(1) = [a_2, a_3, a_4, \dots] \rightarrow \theta(2) = [a_3, a_4, a_5, \dots]$$

so that, given  $\theta(0)$ ,  $\theta(n)$  is nothing but  $\theta(0)$  with the first  $(n-1)$  binary digits removed.<sup>7</sup> This means that any small difference in the less significant digits will be

<sup>6</sup>The Bernoulli map and the tent map are also topologically conjugated but through a complicated non differentiable function (see, e.g., Beck and Schlögl, 1997).

<sup>7</sup>The reader may object that when  $\theta(0)$  is a rational number, the resulting trajectory  $\theta(n)$  should be rather trivial and non-chaotic. This is indeed the case. For example, if  $\theta(0) = 1/4$  i.e. in binary representation  $\theta(0) = [0, 1, 0, 0, 0, \dots]$  under the action of (3.9) will end in  $\theta(n > 1) = 0$ , or  $\theta(0) = 1/3$  corresponding to  $\theta(0) = [0, 1, 0, 1, 0, 1, 0, \dots]$  will give rise to a period-2 orbit, which expressed in decimal is  $\theta(2k) = 1/3$  and  $\theta(2k+1) = 2/3$  for any integer  $k$ . Due to the fact that rationals are infinitely many, one may wrongly interpret the above behavior as an evidence

amplified by the shift operation by a factor 2 at each iteration. Therefore, considering two trajectories,  $\theta(n)$  and  $\theta'(n)$  initially almost equal but for an infinitesimal amount  $\delta\theta(0) = |\theta(0) - \theta'(0)| \ll 1$ , their distance or the error we commit by using one to predict the other will grow as

$$\delta\theta(n) = 2^n \delta\theta(0) = \delta\theta(0) e^{n \ln 2}, \quad (3.10)$$

i.e. exponentially fast with a rate  $\lambda = \ln 2$  which is the *Lyapunov exponent* — the suitable indicator for quantifying chaos, as we will see in Chapter 5.

Let us now go back to the tent map (3.8). For  $\theta(n) < 1/2$  it acts as the shift map, while for  $\theta(n) > 1/2$  the shift is composed with another unary operation that is *negation*,  $\neg$  in symbols, which is defined by  $\neg 0 = 1$  and  $\neg 1 = 0$ . For example, consider the initial condition  $\theta(0) = 0.875 = [1, 1, 1, 0, 0, 0, \dots]$  then  $\theta(1) = 0.25 = [0, 0, 1, 1, 1, \dots] = [\neg 1, \neg 1, \neg 0, \neg 0, \dots]$ . In general, one has  $\theta(0) = [a_1, a_2, \dots] \rightarrow \theta(1) = [a_2, a_3, \dots]$  if  $\theta(0) < 1/2$  (i.e.  $a_1 = 0$ ) while  $\rightarrow \theta(1) = [\neg a_2, \neg a_3, \dots]$  if  $\theta(0) > 1/2$  (i.e.  $a_1 = 1$ ). Since  $\neg^0$  is the identity ( $\neg^0 a = a$ ), we can write

$$\theta(1) = [\neg^{a_1} a_2, \neg^{a_1} a_3, \dots]$$

and therefore

$$\theta(n) = [\neg^{(a_1+a_2+\dots+a_n)} a_{n+1}, \neg^{(a_1+a_2+\dots+a_n)} a_{n+2}, \dots].$$

It is then clear that Eq. (3.10) also holds for the tent map and hence, thanks to the topological conjugacy (Box B.3), the same holds true for the logistic map.

The tent and shift maps are *piecewise linear maps* (see next Chapter), i.e. with constant derivative within sub-intervals of  $[0:1]$ . It is rather easy to recognize (using the graphical construction or linear analysis) that for chaos to be present at least one of the slopes of the various pieces composing the map should be in absolute value larger than 1.

Before concluding this section it is important first to stress that the relation between the logistic and the tent map holds only for  $r = 4$  and second to warn the reader that the behavior of the logistic map, in the range  $r_\infty < r < 4$ , is a bit more complicated than one can expect. This is clear by looking at the so-called *bifurcation diagram (or tree)* of the logistic map shown in Fig. 3.5. The figure is obtained by plotting, for several  $r$  values, the  $M$  successive iterations of the map (here  $M = 200$ ) after a transient of  $N$  iterates (here  $N = 10^6$ ) is discarded. Clearly, such a bifurcation diagram allows periodic orbits (up to period  $M$ , of course) to be identified. In the diagram, the higher density of points corresponds to values of  $r$  for which either periodic trajectories of period  $> M$  or chaotic ones are present. As of the triviality of the map. However, we know that, although infinitely many, rationals have zero Lebesgue measure, while irrationals, corresponding to the *irregular* orbits, have measure 1 in the unit interval  $[0:1]$ . Therefore, for almost all initial conditions the resulting trajectory will be irregular and chaotic in the sense of Eq. (3.10). We end this footnote remarking that rationals correspond to infinitely many (unstable) periodic orbits embedded in the dynamics of the Bernoulli shift map. We will come back to this observation in Chapter 8 in the context of *algorithmic complexity*.

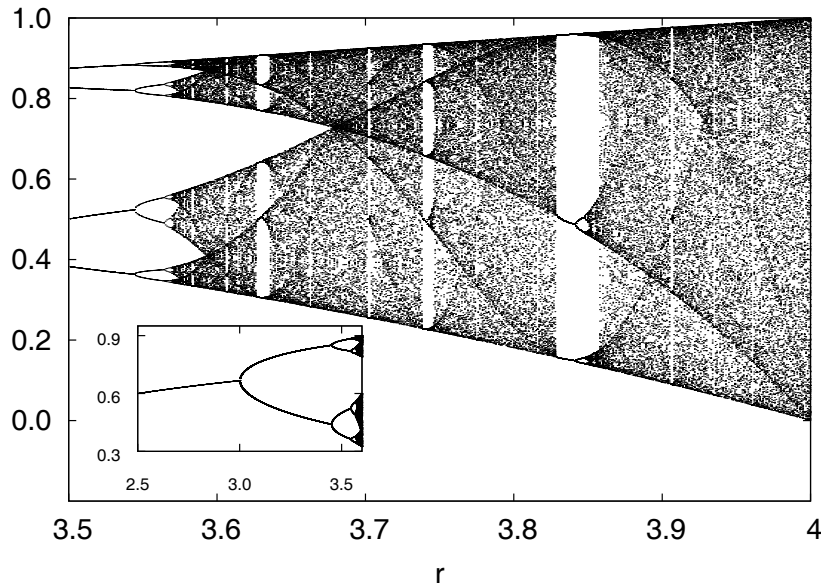


Fig. 3.5 Logistic map bifurcation tree for  $3.5 < r < 4$ . The inset shows the period-doubling region,  $2.5 < r < 3.6$ . The plot is obtained as explained in the text.

readily seen in the figure, for  $r > r_\infty$ , there are several windows of regular (periodic) behavior separated by chaotic regions. A closer look, for instance, makes possible to identify also regions with stable orbits of period-3 for  $r \approx 3.828\dots$ , which then bifurcate to period-6, 12 etc. orbits. For understanding the origin of such behavior one has to study the graphs of  $f_r^{(3)}(x)$ ,  $f_r^{(6)}(x)$  etc.

We will come back to the logistic map and, in particular, to the period doubling bifurcation in Sec. 6.2.

### Box B.3: Topological conjugacy

In this Box we briefly discuss an important technical issue. Just for the sake of notation simplicity, consider the one-dimensional map

$$x(0) \rightarrow x(t) = S^t x(0) \quad \text{where} \quad x(t+1) = g(x(t)) \quad (\text{B.3.1})$$

and the (invertible) change of variable

$$x \rightarrow y = h(x)$$

where  $dh/dx$  does not change sign. Of course, we can write the time evolution of  $y(t)$  as

$$y(0) \rightarrow y(t) = \tilde{S}^t y(0) \quad \text{where} \quad y(t+1) = f(y(t)), \quad (\text{B.3.2})$$